PLASMAS IN THE LABORATORY AND IN THE UNIVERSE

New Insights and New Challenges

Como, Italy 2003

EDITORS
Giuseppe Bertin
Daniela Farina
Roberto Pozzoli

AMERICAN INSTITUTE OF PHYSICS

AIP CONFERENCE PROCEEDINGS ■ 703

Editors:

Giuseppe Bertin
Dipartimento di Fisica
Università degli Studi di Milano
via Celoria 16
20133 Milano
ITALY

E-mail: giuseppe.bertin@unimi.it

Daniela Farina
Istituto di Fisica del Plasma "P. Caldirola"
Consiglio Nazionale delle Ricerche
via R. Cozzi 53
20125 Milano
ITALY

E-mail: farina@ifp.cnr.it

Roberto Pozzoli
Dipartimento di Fisica
Università degli Studi di Milano
via Celoria 16
20133 Milano
ITALY

E-mail: roberto.pozzoli@unimi.it

L.C. Catalog Card No. 2004102021
ISBN 0-7354-0176-4
ISSN 0094-243X
Printed in the United States of America

Free-free absorption effects on Eddington luminosity

L. Ciotti* and J.P. Ostriker†

*Astronomy Department, Bologna University, Italy
†IoA, Cambridge, UK and Dept. of Astrophys. Sciences, Princeton University, NJ, USA

Abstract. In standard treatments the Eddington luminosity is calculated by assuming that the electron-photon cross section is well described by the Thomson cross section which is gray (frequency independent). Here we discuss some consequence of the introduction of free-free opacity in the Eddington luminosity computation: in particular, due to the dependence of bremsstrahlung emission on the *square* of the gas density, it follows that the associated absorption cross section increases *linearly* with the gas density, so that in high density environments Eddington luminosity is correspondingly reduced. We present a summary of an ongoing exploration of the parameter space of the problem, and we conclude that Eddington luminosity in high density environments can be lowered by a factor of ten or more, making it considerably easier for black holes to accelerate and eject ambient gas.

INTRODUCTION

The Eddington luminosity plays a fundamental role in our understanding of accretion phenomena and, as a consequence, of the AGN physics and evolution. In turn, it is also clear that AGNs played a central role in galaxy formation, as testified by several empirical scaling relations between the mass of the supermassive BHs at the center of stellar spheroids (i.e., bulges and elliptical galaxies) and global properties of the spheroids themselves. In standard treatments Eddington luminosity is calculated by assuming that the electron-photon cross section is well described by the *electron scattering* Thompson cross section. Here we discuss the modifications to this simple picture by taking into account *bremsstrahlung* opacity also: due to the dependence of bremsstrahlung emission on the *square* of the gas density, it follows that the associated absorption cross section increases *linearly* with the gas density, so that Eddington luminosity is correspondingly reduced. It is then expected that this opacity source will be important in the range spanned by *cold accretion solutions* (see, Park & Ostriker 1999). These high-density conditions were certainly present at the epoch of galaxy formation, thus a quantitative estimate of the reduction of Eddington luminosity as a function of ambient gas density and temperature is of direct interest when modeling the early stages of galaxy formation (see, e.g., Haiman, Ciotti & Ostriker 2003). In the following discussion we often refer to formulae provided in Ciotti, Ostriker & Pellegrini (2003, hereafter COP): eq. (1) there will be indicated as COP1, and so on.

CP703, *Plasmas in the Laboratory and in the Universe*, edited by G. Bertin, D. Farina, and R. Pozzoli

THE EFFECT OF FREE-FREE ABSORPTION

Let $L_{\rm BH} \equiv \varepsilon \dot{M}_{\rm BH} c^2$ be the bolometric luminosity associated with an accretion rate of $\dot{M}_{\rm BH}$, where ε is the accretion efficiency and c is the speed of light. The *momentum transfer* to the gas electrons per unit time, frequency and volume at the radius r is given by (e.g., see Krolik 1999):

$$\frac{\Delta p}{\Delta t} = \frac{N_{\gamma \rm e}(\nu)}{\Delta t} \times \frac{h\nu}{c} = \frac{L_{\rm BH}(r,\nu)\sigma_{\rm t}(\nu) n_{\rm e}(r)}{4\pi r^2 c}, \tag{1}$$

where $N_{\gamma \rm e}(\nu)$ is the number of photon–electron interactions as given in COP1, $n_{\rm e}(r)$ is the electron number density, h is the Planck constant, and $\sigma_{\rm t}$ is the total electron cross–section corresponding to the various absorption processes (e.g., see Krolik 1999). For simplicity we restrict to the *optically thin regime*: as a consequence, from now on we assume $L_{\rm BH}(r,\nu) \equiv L_{\rm BH} \times f_{\rm BH}(\nu)$ (see COP). The net acceleration field experienced by the accreting gas with density profile $\rho(r)$ is given by $g_{\rm eff}(r) = -GM_{\rm BH}/r^2 + \int_0^\infty (\Delta p/\Delta t) d\nu/\rho(r)$ where G is the gravitational constant. By imposing $g_{\rm eff} = 0$ one obtains

$$L_{\rm Edd} \equiv \frac{\rho(r)}{n_{\rm e}(r)} \frac{4\pi G c M_{\rm BH}}{\int_0^\infty \sigma_{\rm t}(\nu) f_{\rm BH}(\nu) d\nu} : \tag{2}$$

when $\sigma_{\rm t} = \sigma_{\rm T} = 8\pi q_{\rm e}^4/3m_{\rm e}^2 c^4 \simeq 6.65 \times 10^{-25}$ cm^2, the classical expression for $L_{\rm Edd}$ is recovered. Here we consider two different opacity sources for the emitted photons. The first is due to *electron scattering* as described by the Klein–Nishina cross section $\sigma_{\rm KN}(\nu) = \sigma_{\rm T}\tilde{\sigma}_{\rm KN}(x)$, where $x \equiv \nu/\nu_{\rm T}$ and $\nu_{\rm T} \equiv m_{\rm e}c^2/h$ (see COP2). The second is due to *free–free* absorption: its cross cross section $\sigma_{\rm ff}$ is obtained from the bremsstrahlung emission formula (per unit volume, frequency, over the solid angle, Spitzer 1978, hereafter S78)

$$j_{\rm ff}(\nu) = \frac{2^{11/2}(\pi/3)^{3/2} n_{\rm e} q_{\rm e}^6 \sum_i n_{\rm i} Z_i^2 g_{\rm ff.i}}{m_{\rm e}^2 c^4} \left(\frac{m_{\rm e}c^2}{k_{\rm B}T}\right)^{1/2} \exp\left(-\frac{h\nu}{k_{\rm B}T}\right) \tag{3}$$

and the *Kirchhoff's law* $j_{\rm ff}(\nu) = \kappa_{\rm ff} B_\nu(T)$, where $B_\nu(T) = 8\pi h\nu^3 c^{-2}/[\exp(h\nu/k_{\rm B}T) - 1]$ and $k_{\rm B}$ is the Boltzmann constant. Accordingly,

$$\sigma_{\rm ff}(\nu) \equiv \frac{\kappa_{\rm ff}}{n_{\rm e}} = \sigma_{\rm T} \frac{q_{\rm e}^2 c^2 < g_{\rm ff} > \sum_i n_{\rm i} Z_i^2}{\sqrt{6\pi} h} \sqrt{\frac{m_{\rm e}c^2}{k_{\rm B}T}} \frac{1 - \exp(-h\nu/k_{\rm B}T)}{\nu^3}, \tag{4}$$

where $< g_{\rm ff} >$ is the mean *free-free Gaunt factor*. We assume that a mass fraction X of the accreting material is made of fully ionized hydrogen, and the remaining fraction $Y = 1 - X$ by fully ionized helium. Thus, $n_{\rm H} = X\rho/m_{\rm p}$, $n_{\rm He} = (1-X)\rho/4m_{\rm p}$, $n_{\rm e} = (1+X)\rho/2m_{\rm p}$, $n_{\rm t} = (3+5X)\rho/4m_{\rm p}$, and finally $\sum_{i=1}^2 n_{\rm i} Z_i^2 = \rho/m_{\rm p}$. *In other words, at variance with the standard electron scattering case, $\sigma_{\rm ff}$ depends (linearly) on the gas density.* As in COP, we also adopt a (normalized) spectral distribution made by the sum of *two* distinct contributions

$$f_{\rm BH}(\nu) = \frac{f_{\rm X} + \mathscr{R} f_{\rm UV}}{1 + \mathscr{R}}. \tag{5}$$

f_X describes a (normalized) *double-slope*, non thermal distribution of total luminosity L_X, with low and high-frequency slopes ξ_1 and $\xi_1+\xi_2$, respectively, and break frequency ν_b (COP9). f_{UV} is a normalized *black–body* distribution of temperature T_{UV} and total luminosity $L_{UV}\equiv\mathscr{R}L_X$ (COP10); thus $L_{BH}=L_X+L_{UV}=(1+\mathscr{R})L_X$. Accordingly, we study

$$\frac{L_{\rm Edd}^{\rm es}}{L_{\rm Edd}^{\rm es+ff}}=1+\frac{\int_0^\infty\sigma_{\rm ff}f_Xd\nu+\mathscr{R}\int_0^\infty\sigma_{\rm ff}f_{UV}d\nu}{\int_0^\infty\sigma_{\rm KN}f_Xd\nu+\mathscr{R}\int_0^\infty\sigma_{\rm KN}f_{UV}d\nu}. \tag{6}$$

We now compute the four integrals appearing in eq. (6) for some representative values of the parameters entering $f_{BH}(\nu)$. As in COP, we fix $\xi_1=0.9$ and $\xi_2=0.7$, and $\mathscr{R}\simeq 1-2$, so reproducing the observed Compton temperature in quasar spectra (see, e.g., Krolik 1999; Sazonov, Ostriker & Sunyaev 2003). We obtain

$$\int_0^\infty\sigma_{\rm KN}f_Xd\nu\simeq 0.79\left(\frac{\nu_b}{\nu_T}\right)^{-0.05}\sigma_T \tag{7}$$

as a very good fit over the range $0.1\leq\nu_b/\nu_T\leq 10$. The estimate of $\int_0^\infty\sigma_{\rm KN}f_{UV}d\nu$ is trivial: in fact, the 99% of L_{UV} is emitted at $h\nu<10k_BT_{UV}\ll h\nu_T$ for any reasonable value of T_{UV}. Thus $\sigma_{\rm KN}\sim\sigma_T$, and from the normalization condition

$$\int_0^\infty\sigma_{\rm KN}f_{UV}d\nu\simeq\sigma_T. \tag{8}$$

We then obtain

$$\int_0^\infty\sigma_{\rm ff}f_{UV}d\nu=\frac{\rho\sigma_T}{m_p}\frac{15h^2q_e^2c^2<g_{\rm ff}>}{\sqrt{6}\pi^{9/2}k_B^3T_{UV}^3}\sqrt{\frac{m_ec^2}{k_BT}}\int_0^\infty\frac{1-\exp(-\alpha x)}{\exp(x)-1}dx, \tag{9}$$

where $\alpha\equiv T_{UV}/T$, and the dimensionless integral equals $\gamma+\Psi(1+\alpha)$, with $\gamma=0.5772...$ and $\Psi(x)\equiv d\ln\Gamma(x)/dx$. Note that if $T_{UV}=T$ then the integral equals 1; moreover, $\gamma+\Psi(1+\alpha)\sim\pi^2\alpha/6$ for $\alpha\to 0$ and $\Psi(1+\alpha)\sim\ln(\alpha)$ when $\alpha\to\infty$. Thus we have

$$\int_0^\infty\sigma_{\rm ff}f_{UV}d\nu\simeq\frac{\rho\sigma_T}{m_p}\times\begin{cases}\dfrac{1.52\times 10^2}{T_{UV}^2T^{3/2}}, & T_{UV}\lesssim T,\\[2ex] \dfrac{0.93\times 10^2}{T_{UV}^3T^{1/2}}\left(\gamma+\ln\dfrac{T_{UV}}{T}\right), & T_{UV}\gg T,\end{cases} \tag{10}$$

where temperatures are in Kelvin, and we assumed $<g_{\rm ff}>\simeq 9.8$ (see S78). The integral $\int_0^\infty\sigma_{\rm ff}f_Xd\nu$ is affected by a formal infrared divergency if (as in our case) $f_X\sim\nu^{-\xi_1}$ with $\xi_1\geq -1$: in fact, $\sigma_{\rm ff}\sim\nu^{-2}$ for $\nu\to 0$. In order to have a proper physical description we integrate only at frequencies $\nu\geq\chi\nu_p$, where

$$\nu_p\equiv\sqrt{\frac{n_eq_e^2}{\pi m_e}}\simeq 6.35\times 10^3\sqrt{\frac{(1+X)\rho}{m_p}}\quad {\rm s}^{-1} \tag{11}$$

is the plasma frequency. Under the condition $1 \ll \chi \ll k_B T/h\nu_p$, the opacity contribution comes mainly from the Rayleigh-Jeans regime in eq. (4), and the asymptotic value of the integral is

$$\int_{\chi\nu_p}^{\infty} \sigma_{ff} f_X d\nu \sim \frac{7.8\times 10^{12}}{\chi^{1.9}(1+X)^{0.95}T^{3/2}} \left(\frac{\nu_b}{\nu_T}\right)^{-0.1} \left(\frac{\rho}{m_p}\right)^{0.05} \sigma_T. \tag{12}$$

Thus, if $X = 0.75$, $\nu_b/\nu_T = 0.5$, $\mathscr{R} = 2$ and $T_{UV} = T$ we obtain

$$\frac{L_{Edd}^{es}}{L_{Edd}^{es+ff}} \simeq 1 + \frac{1.7\times 10^{12}}{\chi^{1.9}T^{3/2}} \left(\frac{\rho}{m_p}\right)^{0.05} + \frac{50}{T^{7/2}}\frac{\rho}{m_p}. \tag{13}$$

For $T \gtrsim 10^4$ K the free-free opacity contribution to Eddington luminosity is fully dominated by the low frequency tail in the non-thermal spectral distribution. For example, a reduction factor of Eddington luminosity of the order of 10 is obtained for $\chi \simeq 300$ and $\chi \simeq 15$, when $T = 10^5$ K and $T = 10^6$ K, respectively.

Of course, the present analysis leaves open several questions, such as the astrophysical status of the high-density gas at low temperatures, the characteristic linear scale over which the gas becomes optically thick, and the detailed shape of the non-thermal radiation distribution in AGNs at (very) low frequencies. All these aspects of the problem should be proprerly addressed when applying the present results to numerical models.

ACKNOWLEDGMENTS

We thank Giuseppe Bertin, Bruno Coppi, and Bruce Draine for enlightening comments; L.C. aknolwedges the warm hospitality of Princeton University Observatory and the Institute of Astronomy at Cambridge, where a large part of this work was carried out. L.C. was partially supported by a grant CoFin 2000 of the Italian MIUR and by the grant ASI I/R/105/00.

REFERENCES

1. Ciotti, L. Ostriker, J.P, & Pellegrini, S., these Proceedings (COP)
2. Haiman, Z., Ciotti, L. & Ostriker, J.P. 2003, preprint, astro/ph-0304129
3. Krolik, J.H. 1999, *Active galactic nuclei*, Princeton University Press (Princeton, NJ, USA)
4. Park, M.-G., & Ostriker, J.P. 1999, Astroph. J., 527, 247
5. Sazonov, S.Y., Ostriker, J.P. & Sunyaev R.A. 2003, preprint, astro/ph-0305233
6. Spitzer, L. Jr. 1978, *Physical processes in the interstellar medium*, John Wiley & sons (New York) (S78)

Self-consistent stellar dynamical tori

L. Ciotti*, G. Bertin† and P. Londrillo**

*Astronomy Department, Bologna University, Italy
†Physics Department, Milano University, Italy
**INAF-Bologna Astronomical Observatory, Italy

Abstract. We present preliminary results on a new family of distribution functions that are able to generate axisymmetric, truncated (i.e., finite size) stellar dynamical models characterized by *toroidal* shapes. The relevant distribution functions generalize those that are known to describe polytropic spheres, for which all the dynamical and structural properties of the system can be expressed in explicit form as elementary functions of the system gravitational potential. The model construction is then completed by a numerical study of the associated Poisson equation. We note that our axisymmetric models can also include the presence of an external gravitational field, such as that produced by a massive disk or by a central mass concentration (e.g., a supermassive black hole).

INTRODUCTION

Constructing self-consistent collisionless equilibrium models is a key step to understand the structure and the dynamics of stellar systems. The construction process usually starts with the assignment of a phase-space distribution function (DF) obeying the Jeans theorem (and thus a solution of the collisionless Boltzmann equation that describes such "gravitational plasma"), which leads to an expression for the density as a function of the potential; models are then calculated by solving the Poisson equation, as a non-linear, second-order partial differential equation for the potential. In the presence of special symmetries (for example, in the case of spherical models) the problem can be reduced to the study of an ordinary differential equation, and the model construction is relatively straightforward. For more general symmetries the procedure is inherently difficult. In general, solutions have to be found numerically and turn out to exist only for a finite range of the parameters appearing in the adopted DF.

Here we present the basic properties of the simplest member of a new family of DFs that are able to generate axisymmetric, truncated (i.e., finite size) stellar dynamical models characterized by *toroidal* shapes. The complete description of our family of DFs, together with the results of N-body simulations aimed at the study of the *stability* of these collisionless equilibrium configurations, will be presented in a separate paper (Ciotti, Bertin, Londrillo 2004). We recall that toroidal, self-consistent models are sometimes mentioned in the literature (e.g., see Lynden-Bell 1962; the Author expressed concerns about their stability). With our models we will investigate this matter further, also considering the possible stabilizing effect of a massive dark matter halo. Astrophysical applications will address the modeling of *peanut-shaped* bulges (e.g., see Aronica et al. 2003, and references therein) and the problem of the *central depression* recently

CP703, *Plasmas in the Laboratory and in the Universe*, edited by G. Bertin, D. Farina, and R. Pozzoli

discovered (Lauer et al. 2002) in the luminosity profiles of some elliptical galaxies hosting supermassive black holes.

THE MODELS

The particular set of axisymmetric models presented here is defined by the DF

$$f(Q,J_z^2) = f_0|J_z|^{2\alpha}(Q-Q_0)^{\beta}\Theta(Q-Q_0), \tag{1}$$

where f_0 is a (dimensional) physical scale, $Q \equiv \mathscr{E} - J_z^2/(2R_a^2)$, Θ is the Heaviside step function, and α and β are two dimensionless constants; the natural coordinates are cylindrical, (R,z,φ). In addition, $\mathscr{E} \equiv \Psi_T - ||\mathbf{v}||^2/2 = \Psi_T - (v_R^2 + v_z^2 + v_\varphi^2)/2$ is the binding energy per unit mass, $J_z = Rv_\varphi$ is the axial component of the angular momentum (per unit mass), and Q_0 and R_a are a *truncation energy* and an *anisotropy radius*, respectively. The function $\Psi_T = \Psi_T(R,z)$ represents the total gravitational potential; for the moment, we only require that $\Psi_T \sim O(r^{-1})$ for $r \to \infty$, where $r = \sqrt{R^2+z^2}$. We allow for an external component also, i.e., $\Psi_T = \Psi + \Psi_{ext}$, where Ψ is the potential associated with the density distribution derived from eq. (1) as given by the following eq. (4), while Ψ_{ext} is taken to be a given function (equal to zero in the fully self-consistent case). Note that we can write

$$Q = \Psi_T - \frac{v_m^2}{2} - \frac{v_\varphi^2}{2}\left(1+\frac{R^2}{R_a^2}\right), \tag{2}$$

where $v_m^2 \equiv v_R^2 + v_z^2$ is the square of the meridional (or poloidal) velocity component. Some dynamical properties of the systems associated with eq. (1) are the following: (*i*) no net rotation is present, and (*ii*) the two components σ_R^2 and σ_z^2 of the velocity dispersion tensor are equal. In addition, note that for $\alpha = 0$ if we formally consider $R_a \to \infty$ we recover the polytropic spheres, while for integer α and β the distribution function is a *sum* of Fricke's (1952) DFs. The functional dependence of the system structural and dynamical properties on Ψ_T is obtained by integration over $\Omega(\mathbf{x})$, the velocity section of phase–space over which $f \geq 0$ at given $\mathbf{x}$. The coordinates (v,ζ,ξ) to be used to integrate the various quantities over the rotationally symmetric (ellipsoidal) region $\Omega(\mathbf{x})$ are naturally defined by

$$v_R = v\sin\zeta\cos\xi, \quad v_z = v\sin\zeta\sin\xi, \quad v_\varphi = \frac{v\cos\zeta}{\sqrt{1+R^2/R_a^2}}, \tag{3}$$

where $0 \leq \zeta \leq \pi$, $0 \leq \xi \leq 2\pi$. With this choice, the ellipsoidal radius v of the velocity section $\Omega(\mathbf{x})$ runs in the range $0 \leq v \leq \sqrt{2[\Psi_T(\mathbf{x}) - Q_0]}$. Integration over the two angular coordinates gives

$$\rho = 4\pi f_0 g(R)\frac{B(\alpha+3/2,\beta+1)2^{\alpha+1/2}}{2\alpha+1}(\Psi_T - Q_0)^{\alpha+\beta+3/2}\Theta(\Psi_T - Q_0), \tag{4}$$

where $B(x,y) = \int_0^1 t^{x-1}(1-t)^{y-1}dt$ is the Euler Beta function,

$$g(R) = \frac{R^{2\alpha}}{(1+R^2/R_a^2)^{\alpha+1/2}}, \tag{5}$$

and for convergence it is required that $\alpha > -1/2$, $\beta > -1$. Moreover,

$$\rho\sigma_m^2 = 4\pi f_0 g(R) \frac{B(\alpha+5/2,\beta+1)2^{\alpha+5/2}}{(2\alpha+1)(2\alpha+3)}(\Psi_T - Q_0)^{\alpha+\beta+5/2}\Theta(\Psi_T - Q_0) \tag{6}$$

and

$$\rho\sigma_\varphi^2 = \frac{4\pi f_0 g(R)}{1+R^2/R_a^2}\frac{B(\alpha+5/2,\beta+1)2^{\alpha+3/2}}{2\alpha+3}(\Psi_T - Q_0)^{\alpha+\beta+5/2}\Theta(\Psi_T - Q_0). \tag{7}$$

The number of free parameters (excluding those associated with the external potential) needed to describe a model completely is five: the three dimensional quantities f_0, R_a, and Q_0, and the two dimensionless constants α and β. The relation between the meridional velocity dispersion σ_m^2 and the azimuthal (toroidal) velocity dispersion σ_φ^2, can be described by the anisotropy distribution

$$a(R,z) \equiv 1 - \frac{2\sigma_\varphi^2}{\sigma_m^2} = \frac{R^2/R_a^2 - 2\alpha}{R^2/R_a^2 + 1}. \tag{8}$$

The velocity dispersion tensor is isotropic when $a = 0$, tangentially anisotropic when $a < 0$, and meridionally anisotropic when $a > 0$. Note that the velocity dispersion anisotropy is constant on *cylinders*. It can be proved that eq. (8) holds also when the factor $(Q - Q_0)^\beta$ in eq. (1) is replaced by a generic function $h(Q - Q_0)$ (Ciotti et al. 2004). We now impose the system consistency, i.e., we require that

$$\triangle\Psi = -4\pi G\rho, \tag{9}$$

with Ψ a nowhere negative function. In order to obtain the numerical solution of eq. (9), the Poisson equation is first recast in dimensionless form, by referring to the physical scales R_a for lengths and Q_0 for potentials. After rescaling, we are then led to the solution of the following problem:

$$\tilde{\triangle}\phi = -\lambda\tilde{\rho}, \qquad \tilde{\rho} \equiv g(\tilde{R})(\phi_T - 1)^\gamma\Theta(\phi_T - 1), \tag{10}$$

where $\gamma \equiv \alpha+\beta+3/2 > 0$, and the dimensionless quantities are defined as $\phi_T \equiv \Psi_T/Q_0$, $\tilde{R} \equiv R/R_a$, and $g(\tilde{R}) \equiv \tilde{R}^{2\alpha}/(1+\tilde{R}^2)^{\alpha+1/2}$, with

$$\lambda \equiv \frac{16\pi^2 G f_0 R_a^{2\alpha+2} Q_0^{\alpha+\beta+1/2} B(\alpha+3/2,\beta+1)2^{\alpha+1/2}}{2\alpha+1}. \tag{11}$$

It follows that

$$\rho = \frac{Q_0}{GR_a^2}\frac{\lambda\tilde{\rho}}{4\pi} \tag{12}$$

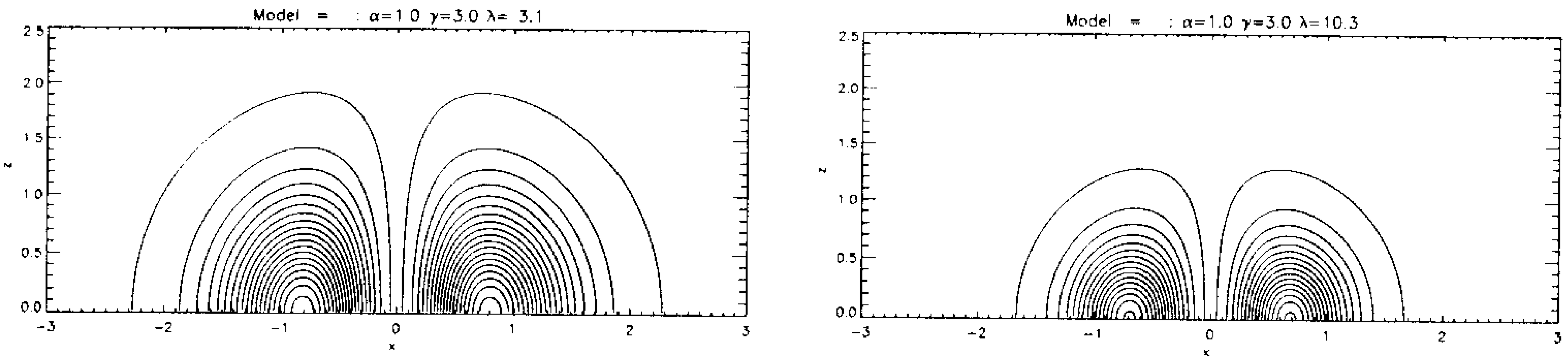

FIGURE 1. Isodensity contours of a meridional section of the dimensionless density distribution associated with the models $(\alpha,\gamma) = (1,3)$ for $\lambda \simeq 3.1$ (left) and $\lambda \simeq 10.3$ (right).

and

$$\tilde{\sigma}_{\rm m}^2 = \frac{2}{\gamma+1}(\phi_{\rm T}-1)\Theta(\phi_{\rm T}-1), \quad \tilde{\sigma}_{\varphi}^2 = \frac{2\alpha+1}{(\gamma+1)}\frac{(\phi_{\rm T}-1)\Theta(\phi_{\rm T}-1)}{1+\tilde{R}^2}. \tag{13}$$

Equation (10), a classical non-linear elliptic partial differential equation, is then solved by using a Newton iteration scheme, described in detail by Ciotti et al. (2004). In general, for assigned model parameters we found convergence only for finite intervals of λ. In Figure 1 we show the meridional sections of the density distribution of two representative truncated and fully self-consistent ($\Psi_{\rm ext} = 0$) toroidal models, obtained by fixing $\alpha > 0$ (see eqs. [5] and [10]), for two different values of λ.

ACKNOWLEDGMENTS

The work of G.B. and L.C. has been partially supported by a grant CoFin 2000 of the Italian MIUR.

REFERENCES

1. Aronica, G., Athanassoula, E., Bureau, M., Bosma, A., Dettmar, R.-J., Vergani, D., & Pohlen, M. 2003, Astrophys. Sp. Sci., 284, 753
2. Ciotti, L., Bertin, G., Londrillo, P. 2004, to be submitted to Astron. Astrophys.
3. Fricke, W. 1952, Astron. Nachr., 280, 193
4. Lauer, T., et al. 2002, Astron. J., 124, 1975
5. Lynden-Bell, D. 1962, Mon. Not. Roy. Astron. Soc., 123, 447

The role of Compton heating in cluster cooling flows

L. Ciotti*, J.P. Ostriker† and S. Pellegrini*

*Astronomy Department, Bologna University, Italy
†IoA, Cambridge, UK and Dept. of Astrophys. Sciences, Princeton University, NJ, USA

Abstract. Recent observations by Chandra and XMM-Newton demonstrate that the central gas in "cooling flow" galaxy clusters has a mass cooling rate that decreases rapidly with decreasing temperature. This contrasts the predictions of a steady state cooling flow model. On the basis of these observational results, the gas can be in a steady state only if a steady temperature dependent heating mechanism is present; alternatively the gas could be in an unsteady state, i.e., heated intermittently. Intermittent heating can be produced by accretion on the supermassive black hole residing in the central cluster galaxy, via Compton heating. This mechanism can be effective provided that the radiation temperature of the emitted spectrum is higher than the gas temperature. Here we explore whether this heating mechanism can be at the origin of the enigmatic behavior of the hot gas in the central regions of "cooling flow" clusters. Although several characteristics of Compton heating appear attractive in this respect, we find that the fraction of absorbed heating for realistic gas and radiation temperatures falls short by two orders of magnitude of the required heating.

INTRODUCTION

X-ray observations of the central regions of a large fraction of galaxy clusters prior to *Chandra* and $XMM-Newton$ were interpreted in terms of cooling and condensing of the intracluster medium (ICM), leading to a subsonic, steady central inflow called cooling flow (Cowie & Binney 1977, Fabian & Nulsen 1977). The measurements of radiative cooling times lower than a Hubble time within a cooling radius ($r_{\rm cool}$) of $\lesssim$ few hundreds of kiloparsecs were at the basis of this idea. However, cool gas in the cluster cores (in the form of massive-star formation or formation of low-mass stars, optical emission line nebulae or cold gas) has never been discovered in a quantity large enough to fit with the steady state cooling flow predictions (e.g., Donahue & Voit 2003). Moreover recent observations from the *Chandra* and $XMM-Newton$ satellites have ruled out the simple steady state cooling flow model (e.g., Molendi & Pizzolato 2001, Peterson et al. 2003). In this model one expects emission from gas over the entire temperature range (from $T_{\rm max}$, the ambient ICM temperature, down to temperature values at which the ICM is undetectable in the X-rays), *with the same mass cooling rate* $\dot{M}$ *at each temperature.* The strengths of a few observed emission lines reveal how much gas cools through each temperature, and high resolution spectroscopic observations now show a deficit of emission relative to the cooling flow predictions from gas below $\sim T_{\rm max}/3$ (Peterson et al. 2003). In addition, the spectra show increasingly less emission at lower temperatures than the cooling flow model would predict. Empirically, the differential luminosity distribution $\Delta L/\Delta T \propto T^{1\div 2}$, instead of being temperature-independent as expected in

CP703, *Plasmas in the Laboratory and in the Universe*, edited by G. Bertin, D. Farina, and R. Pozzoli

the radiative cooling flow model. Lower spectral resolution observations, as from the *Chandra* ACIS-S detector, also suggest significantly lower mass cooling rates than obtained from previous analyses of *ROSAT* and *ASCA* data (McNamara et al. 2000).

These observational results have produced an important astrophysical puzzle and a number of ideas have been suggested to solve it, but none has been proven conclusive yet. For example, cooling may be opposed by heating (Soker et al. 2001) or thermal conduction may suppress cooling (Ruskowkski & Begelman 2002). 'Cooling flows' generally have embedded non-thermal radio sources and this association suggests that feedback from an AGN may help suppress the cooling of the ICM. This feedback may come from the impact of the radio jets on the cooling gas (Reynolds et al. 2002, Omma et al. 2003) or from mixing and turbulent heating as buoyant radio plasma rises through the ICM (Brüggen & Kaiser 2002). Another plausible (intermittent) heating source could be Compton heating resulting from accretion of the cooling gas on the central supermassive black hole of the central galaxy in the cluster core. Although the gas over the body of the galaxy is optically thin, numerical simulations showed that this mechanism is very effective in heating the interstellar medium of giant elliptical galaxies (Ciotti & Ostriker 2001). Here we explore whether it can provide effective feedback also in the case of cluster cores.

The bolometric luminosity associated with accretion in the galactic nucleus is $L_{\rm BH} = \varepsilon \dot{M}_{\rm BH} c^2$, where $\dot{M}_{\rm BH}$ is the accretion rate on the black hole, ε is the accretion efficiency (usually spanning the range $0.001 \lesssim \varepsilon \lesssim 0.1$) and c is the speed of light. Taking $\dot{M}_{\rm BH}$ of the order of few 10s of $M_\odot$ yr^{-1}, as suggested by the most recent estimates of the mass accretion rate in 'cooling flows' (Peterson et al. 2003), the power available for heating of the ICM turns out to be $\sim 10^{47}$ erg s^{-1}. The power required to balance the cooling of the ICM in the 'cooling flow' region must be of the order of its observed X-ray luminosity; this goes from $\sim 10^{43}$ erg s^{-1} in the Virgo cluster up to $\sim 10^{45}$ erg s^{-1} in the most massive clusters like A1835. Therefore it seems that during the phases of accretion there could be enough power to balance the cooling. The problem is: How much of $L_{\rm BH}$ is actually *trapped* by the inflowing gas and therefore is effectively available for its heating? It is clear that for extremely low opacities $L_{\rm BH}$ would be unable to affect the flow. In the following we estimate how much of $L_{\rm BH}$ is absorbed by the ICM in the core regions of galaxy clusters, for typical temperature and density profiles.

SETTING THE PROBLEM

The number of photon–electron interactions per unit volume and in the time interval Δt at any radius r in a plasma can be written as:

$$N_{\gamma {\rm e}}(\nu, r) = N_\gamma(\nu, r) \times \frac{\sigma_{\rm KN}(\nu) n_{\rm e}(r)}{4\pi r^2} = \frac{L_{\rm BH}(\nu, r)\Delta t}{h\nu} \times \frac{\sigma_{\rm KN}(\nu) n_{\rm e}(r)}{4\pi r^2}, \qquad (1)$$

where $n_{\rm e}(r)$ is the electron number density, h is the Planck constant and $\sigma_{\rm KN}$ is the Klein-Nishina electron scattering cross-section (Lang 1980):

$$\sigma_{\rm KN}(\nu) = \frac{3\sigma_{\rm T}}{4} \left\{ \frac{1+x}{x^2} \left[\frac{2(1+x)}{1+2x} - \frac{\ln(1+2x)}{x} \right] + \frac{\ln(1+2x)}{2x} - \frac{1+3x}{(1+2x)^2} \right\}, \qquad (2)$$

where $x \equiv \nu/\nu_{\mathrm{T}}$, $\nu_{\mathrm{T}} \equiv m_{\mathrm{e}}c^2/h$ is the Thomson frequency, m_{e} is the electron mass and σ_{T} is the Thomson cross section. Here for simplicity we assume a *gray* absorption, i.e.:

$$L_{\mathrm{BH}}(\nu,r) = f_{\mathrm{BH}}(\nu) \times L_{\mathrm{BH}}(r), \quad \int_0^\infty f_{\mathrm{BH}}(\nu)\,d\nu = 1, \tag{3}$$

where $L_{\mathrm{BH}}(r)$ is the bolometric accretion luminosity that reaches the radius r from the nucleus.

The gas Compton heating (or cooling) per unit frequency at radius r is given by $\Delta E = -N_{\gamma\mathrm{e}}(\nu)\Delta E_\gamma(\nu,T)$, where ΔE is the internal energy per unit volume gained (or lost) by the gas from radiation at frequency ν, and ΔE_γ is the energy variation of a photon of frequency ν interacting with an electron of gas at temperature T. A simple approximation for the energy transfer factor is[1]:

$$\Delta E_\gamma(\nu,T) = \frac{x(1+3x^2/8)}{1+x^3}4k_{\mathrm{B}}T - \frac{x^2(1+x^2)}{1+x^3}m_{\mathrm{e}}c^2 \tag{4}$$

where k_{B} is the Boltzmann constant. After substitution of (1) and (4) in the expression for the Compton heating, and integration over all frequencies, one has:

$$\frac{\Delta E}{\Delta t} = -\frac{n_{\mathrm{e}}(r)}{n_{\mathrm{t}}(r)}\frac{E(r)}{4\pi r^2}\frac{L_{\mathrm{BH}}(r)}{m_{\mathrm{e}}c^2}\frac{8\Gamma_{\mathrm{C}}}{3}\left[1 - \frac{T_{\mathrm{C}}}{T(r)}\right], \tag{5}$$

where $n_{\mathrm{t}}(r)$ is the total number density,

$$\Gamma_{\mathrm{C}} \equiv \int_0^\infty \frac{(1+3x^2/8)f_{\mathrm{BH}}(\nu)\sigma_{\mathrm{KN}}(\nu)}{1+x^3}\,d\nu \tag{6}$$

and the spectral temperature T_{C} is given by:

$$T_{\mathrm{C}} \equiv \frac{m_{\mathrm{e}}c^2}{4k_{\mathrm{B}}\Gamma_{\mathrm{C}}}\int_0^\infty \frac{x(1+x^2)f_{\mathrm{BH}}(\nu)\sigma_{\mathrm{KN}}(\nu)}{1+x^3}\,d\nu, \tag{7}$$

where $m_{\mathrm{e}}c^2/4k_{\mathrm{B}} = 1.48 \times 10^9$ K.

Integrating on r the equation of energy conservation $\partial L_{\mathrm{BH}}(r)/\partial r = -4\pi r^2 \partial E(r)/\partial t$, one has

$$L_{\mathrm{BH}}(r) = L_{\mathrm{BH}}(0)\exp\left\{\frac{8}{3}\frac{\Gamma_{\mathrm{C}}}{m_{\mathrm{e}}c^2}\int_0^r E(r)\frac{n_{\mathrm{e}}(r)}{n_{\mathrm{t}}(r)}\left(1 - \frac{T_{\mathrm{C}}}{T(r)}\right)dr\right\}. \tag{8}$$

From the above equation we can compute the amount of energy actually trapped to heat the gas, for any gas temperature and density profile and any spectral energy distribution of the nuclear photons.

---

[1] This formula reproduces the well known relations $\Delta E_\gamma \sim 1.5k_{\mathrm{B}}T - m_{\mathrm{e}}c^2x + O(1/x)$ for relativistic photon energy ($h\nu \gg m_{\mathrm{e}}c^2$), and $\Delta E_\gamma \sim 4k_{\mathrm{B}}Tx - m_{\mathrm{e}}c^2x^2 + O(x^3)$ in the classical limit ($h\nu \ll m_{\mathrm{e}}c^2$).

We assume that the spectral energy distribution $f_{\rm BH}(\nu)$ is made of two distinct contributions. The first is a non thermal distribution of total luminosity $L_{\rm X}(\nu) = f_{\rm X}(\nu) \times L_{\rm X}$, with

$$f_{\rm X}(\nu) = \frac{\xi_2}{\pi \nu_{\rm T}} \sin\left[\frac{\pi(1-\xi_1)}{\xi_2}\right] \left(\frac{\nu_{\rm b}}{\nu_{\rm T}}\right)^{\xi_1+\xi_2-1} \frac{x^{-\xi_1}}{(\nu_{\rm b}/\nu_{\rm T})^{\xi_2} + x^{\xi_2}}, \qquad (9)$$

where $h\nu_{\rm b}$ is the spectrum break energy and ξ_1 and $\xi_1 + \xi_2$ are the spectral slopes at low and high frequencies. The second is a blackbody distribution $L_{\rm UV}(\nu) = f_{\rm UV}(\nu) \times L_{\rm UV}$ at a temperature $T_{\rm UV}$, with

$$f_{\rm UV}(\nu) = \frac{15h^4}{\pi^4 k_{\rm B}^4 T_{\rm UV}^4} \frac{\nu^3}{\exp(h\nu/k_{\rm B}T_{\rm UV}) - 1} \simeq \frac{8.17 \times 10^{-43}}{T_{\rm UV}^4} \frac{\nu^3}{\exp(h\nu/k_{\rm B}T_{\rm UV}) - 1} \ (s). \qquad (10)$$

For these distributions $\int_0^\infty f_{\rm X}(\nu)d\nu = 1$ and $\int_0^\infty f_{\rm UV}(\nu)d\nu = 1$. We also assume that $L_{\rm UV} \equiv \mathscr{R} L_{\rm X}$, where $\mathscr{R}$ is a dimensionless parameter measuring the relative importance of the "UV bump" with respect to the high energy part of the spectral energy distribution. Following this choice, the frequency distribution of $L_{\rm BH}$ in (3) can be written as

$$f_{\rm BH}(\nu) = \frac{f_{\rm X} + \mathscr{R} f_{\rm UV}}{1 + \mathscr{R}}, \qquad (11)$$

and $L_{\rm BH}(0) = L_{\rm X} + L_{\rm UV} = (1+\mathscr{R})L_{\rm X}$.

THE RESULTS

We first estimate the dependence of $\Gamma_{\rm C}$ and $T_{\rm C}$, i.e., of the integrals in (6) and (7), on the free parameters $T_{\rm UV}$, $\nu_{\rm b}$, ξ_1, ξ_2. We adopt $\xi_1 = 0.9$ and $\xi_2 = 0.7$; these values reproduce the observed spectral shapes of the X–ray and γ–ray emission of AGNs (e.g., Nandra & Pounds 1994; Lu & Yu 1999). The coefficient $\Gamma_{\rm C}$ is evaluated numerically by considering the range $0.1 \leq \nu_{\rm b}/\nu_{\rm T} \leq 10$ for $f_{\rm X}$ and the classical limit for $f_{\rm BH}(\nu)$, i.e., $k_{\rm B}T_{\rm UV} \ll h\nu_{\rm T}$. We obtain

$$\Gamma_{\rm C} \equiv \Gamma_{\rm X} + \mathscr{R}\Gamma_{\rm UV} \simeq \frac{0.77 \times (\nu_{\rm b}/\nu_{\rm T})^{-0.06} + \mathscr{R}}{1+\mathscr{R}} \times \sigma_{\rm T}. \qquad (12)$$

A similar evaluation of the dimensionless integral on the r.h.s. of (7) gives

$$T_{\rm C} \simeq \frac{8.6 \times 10^7 \times (\nu_{\rm b}/\nu_{\rm T})^{0.196} + \mathscr{R} T_{\rm UV}}{0.77 \times (\nu_{\rm b}/\nu_{\rm T})^{-0.06} + \mathscr{R}} \ (K). \qquad (13)$$

For observed values of $\nu_{\rm b}/\nu_{\rm T} \sim 0.2$ and $\mathscr{R} \sim 1$ (e.g., Fabian 1996), $T_{\rm C} = 4 \times 10^7$ K (independently of $T_{\rm UV}$). This value for $T_{\rm C}$ is very similar to that derived by Sazonov et al. (2003) from composite mean QSOs spectra.

We next performed the integration in (8) to estimate $L_{\rm BH}(r) - L_{\rm BH}(0)$, which is the amount of energy actually trapped by the ICM within a radius r. The integration was extended out to the 'cooling radius' ($r_{\rm cool}$), within which a 'cooling flow' could develop.

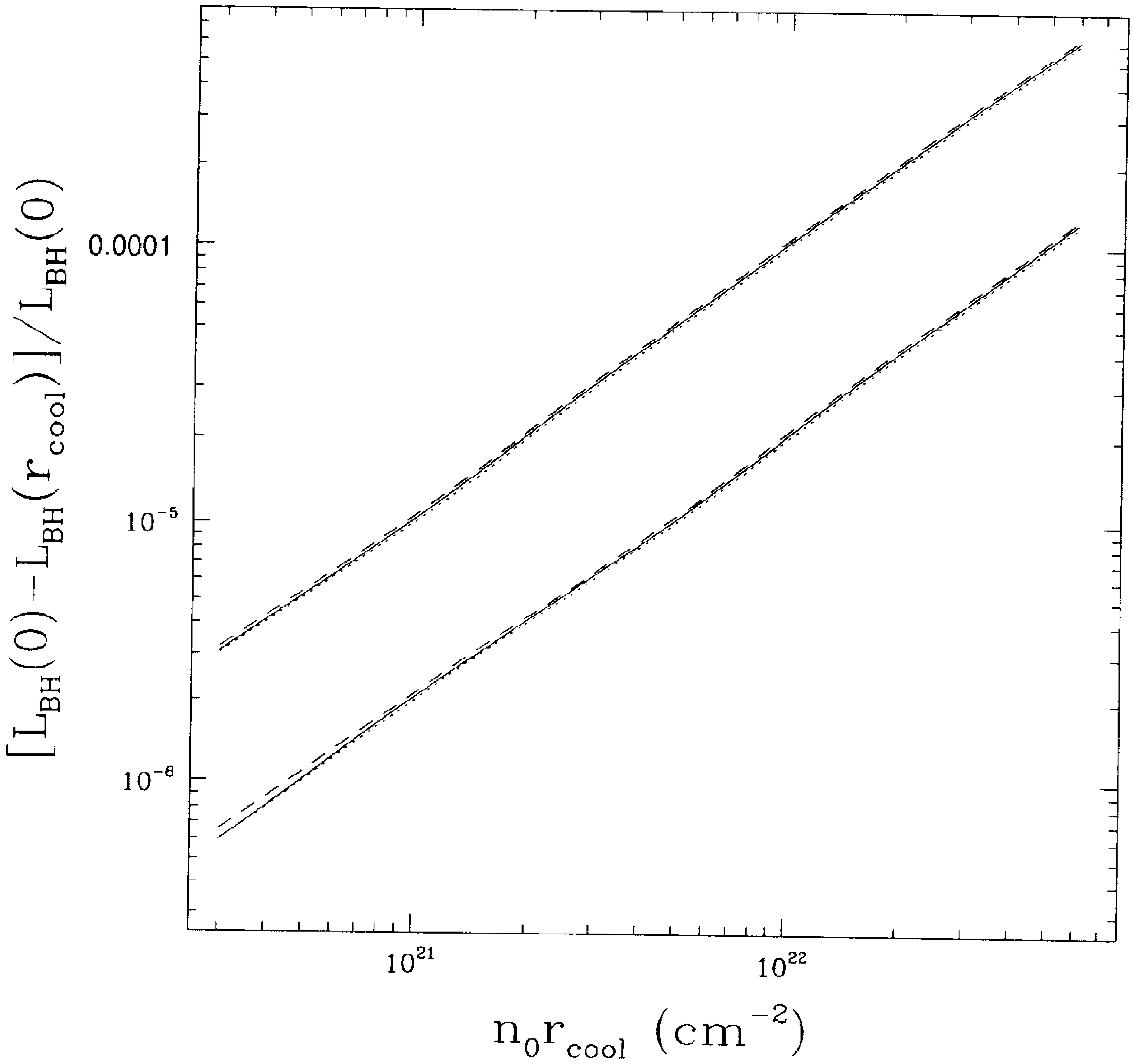

FIGURE 1. The amount of nuclear radiation that actually heats the ICM within $r_{\rm cool}$. ν_b/ν_T is fixed at 0.2. The upper set of curves refers to $T_C - T = 5\times10^7$ K, the lower set to $T_C - T = 10^7$ K. Solid lines refer to $\mathscr{R} = 1$, dashed ones to $\mathscr{R} = 2$ and dotted ones to $\mathscr{R} = 0.5$.

For low T_C values ($\sim 1-2$ keV, as allowed by the study of Sazonov et al. 2003), $r_{\rm cool}$ encloses the only region within which the ICM temperature T is lower than T_C. We assume that the gas is isothermal at a temperature T within $r_{\rm cool}$. The adopted ICM density profile is a deprojection of the $\beta-$model commonly used to reproduce the observed X-ray surface brightness (i.e., Sarazin 1986): $\rho_{\rm gas} = \rho_0[1+(r/r_c)^2]^{-3\beta/2}$, where r_c is the core radius ($\sim$ 250 kpc on average) and ρ_0 is the total particle density at $r=0$. The integration in (8) gives:

$$L_{\rm BH}(r_{\rm cool}) = L_{\rm BH}(0)\exp\left[-\frac{4\Gamma_C}{m_e c^2}\frac{n_e}{n_t}k_B(T_C-T)n_0 r_c f\left(\frac{r_{\rm cool}}{r_c},\beta\right)\right] \qquad (14)$$

where $n_0 = \rho_0/\mu m_p$ with μm_p the average particle mass. For our choice of $r_{\rm cool} \lesssim r_c$, the function $f \approx r_{\rm cool}/r_c$ and is independent of β. This approximate value for the integral is within 25% of the true value, for $\beta = 0.3-0.9$. In Fig. 1 we plot the amount of nuclear radiation that actually heats the ICM within $r_{\rm cool}$ as a function of $n_0 r_{\rm cool}$. The range of variation for $n_0 r_{\rm cool}$ is chosen by considering the observed ranges for $r_{\rm cool}$ (50 – 200 kpc, Peterson et al. 2003) and n_0 ($2 \times 10^{-3} - 0.1$ cm^{-3}). Taking $n_e/n_t = 0.5$, the free parameters left in the expression for $L_{\rm BH}(r_{\rm cool})$ in (14) are v_b/v_T, $\mathscr{R}$ and $T_C - T$. In Fig. 1 we consider a possible range for $\mathscr{R} = 0.5 - 2$ and two extreme cases for the difference $T_C - T$, corresponding to a high T_C value [$\sim (5-6) \times 10^7$ K] and a low one ($T_C \sim 2 \times 10^7$ K). Note that Γ_C varies by $< 10\%$ for $v_b/v_T = 0.1 - 1$, and so the results are totally unaffected by variations of v_b/v_T in this range.

CONCLUSIONS

From Fig. 1 it appears that the power actually available for heating of the ICM within the cooling region goes from few$\times 10^{-6} L_{\rm BH}(0)$, in the small clusters, up to $10^{-4} L_{\rm BH}(0)$ in the most massive ones. This makes Compton heating fall short by $\sim$two orders of magnitude of the required heating and therefore an unplausible mechanism to balance the cooling of the gas in the cluster core, at variance with the situation in elliptical galaxies (Ciotti & Ostriker 2001).

ACKNOWLEDGMENTS

L.C. and S.P. thank the IoA for hospitality and financial support during a visit where most of the results presented here were obtained.

REFERENCES

1. Brüggen, M., Kaiser, C.R. 2002, Nature, 418, 301
2. Ciotti, L., Ostriker, J.P. 2001, Astrophys. J., 551, 131
3. Cowie, L., Binney, J. 1977, Astrophys. J., 215, 723
4. Donahue, M., Voit, M. 2003, astro-ph/0308006
5. Fabian, A.C., Nulsen, P.E.J. 1977, Mon. Not. Roy. Astron. Soc., 180, 479
6. Fabian, A.C. 1996, Proc. 'Roentgenstrahlung from the Universe', eds. Zimmermann, H.U., Truemper, J. and Yorke, H.; MPE Report 263, p. 403–408
7. Lang, K.R. 1980, Astrophysical Formulae, Springer-Verlag Berlin
8. Lu, Y., Yu, Q. 1999, Astrophys. J., 526, L5
9. McNamara, B., et al. 2000, Astrophys. J., 534, L135
10. Molendi, S., Pizzolato, F. 2001, Astrophys. J., 560, 194
11. Nandra, K., Pounds, K.A. 1994, Mon. Not. Roy. Astron. Soc., 268, 405
12. Omma, H., Binney, J., Bryan, G., Slyz, A. 2003, astro-ph/0307471
13. Peterson, J.R., et al. 2003, Astrophys. J., 590, 207
14. Reynolds, C.S., Heinz, S., Begelman, M.C. 2002, Mon. Not. Roy. Astron. Soc., 332, 271
15. Ruskowski, M., Begelman, M.C. 2002, Astrophys. J., 581, 223
16. Sazonov, S.Y., Ostriker, J.P. & Sunyaev, R.A. 2003
17. Soker, N., White, R.E.III, David, L.P., McNamara, B.R. 2001, Astrophys. J., 549, 832